# Characteristics of rail pads tested at laboratory and under track conditions

Helmut Venghaus
ACCON GmbH, Greifenberg Germany.

Martin Toward
Institute of Sound & Vibration Research, University of Southampton, Southampton, England.

Enzo Scossa-Romano
Schweizerische Bundesbahn, Bern, Switzerland.

**Summary**

The influence of rail pads on noise emission of railway tracks is well known, as they couple rail and sleeper. Stiff rail pads will lead to a more direct coupling leading to a higher energy flow from rail to sleeper and resulting in a lower noise radiation of the rail. Although there is a high knowledge about this in some cases a higher noise radiation is measured than it would be estimated by the stiffness of the rail pads. During a R&D-project funded by the Swiss Federal Office for Transport some indicators were identified, that the stiffness of the rail pads will decrease under wear. Beside standard measurements at real track different analysis methods - by measurements at laboratory of demounted pads or by re-calculation from TDR-values - were tried to define the change of aged worn rail pads.

PACS no. **43.90.+v**

## 1. Introduction

Track decay rates are a frequency dependent measure of the attenuation of vibration with distance along a railway track. The rail pads fitted between the rail and sleeper have a strong influence on the decay rates. Measurements of decay rates on some sections of Swiss railway tracks have shown inconsistencies compared to what would be predicted based on the track properties using an analytical track model e.g. [1]. The majority of rail pads used on the Swiss rail network are of the same type. However at some test locations the measured decay rates between 300 Hz and 1 kHz are much lower than would be expected based on the pad stiffness values supplied by the manufacturer. To explore this phenomenon a R&D study by the Swiss Federal Railway Company (SBB) was commissioned in 2014.

Within the ongoing SBB study, noise and vibration measurements have been made at 16 sections of track distributed over the Swiss railway network. Vibration of the rail and sleeper were monitored during train passbys and because most of these locations were situated at the Swiss railway monitoring stations, the radiated noise during these measurements as well as a historical data set of the noise were also available. In addition, at some locations, the roughness and track decay rates of the test sections were measured. After the measurements, at each location four rail pads were taken from the track to be used for additional laboratory tests. These laboratory tests were aimed at understanding whether the inconsistency in the decay rate measurements may have been caused by variations from the expected properties of the rail pads at the sites. The stiffness of the rail pads was obtained using two methods. The first involved measuring their deflection when dynamically loaded using a servo hydraulic actuator at the laboratories of Studiengesellschaft fuer unterirdische Verkehrsanlagen (STUVA) in Cologne. In the second method, the in-situ stiffness of the rail pad was predicted by fitting a track model to the measured track decay rate (TDR) at the sites. This paper presents the finding of these tests rail pads and discusses possible explanations for the inconsistency in the track decay rate measurements.

## 2. Rail pads at SBB tracks

The majority of rail pads used in the Swiss railway network are of the type Zw 661a. These EVA pads



Copyright© (2015) by EAA-NAG-ABAV, ISSN 2226-5147
All rights reserved

have a manufacturer's reported static stiffness of around 700 kN/mm. Generally, 'stiff' pads such as these provide a good coupling of rail and sleeper leading to relatively high track decay rates.

Within this project there was the possibility to compare worn and recently inserted rail pads at one location in Wichtrach (track No.317). This track was completely renewed in 2013. The TDRs were measured before the renewal and the 30 year old rail pads were stored. In 2014 – after nearly half a year in duty – the track decay rates were measured again. Figures 1 and 2 display the vertical and lateral decay rates for the old and new track.

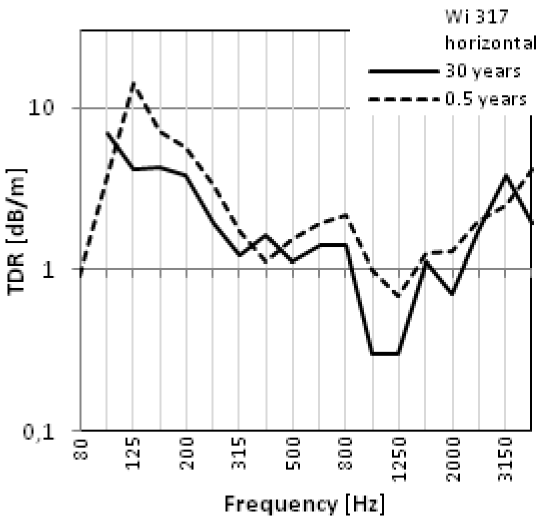


Figure 1 Horizontal TDRs of worn and new rail pads

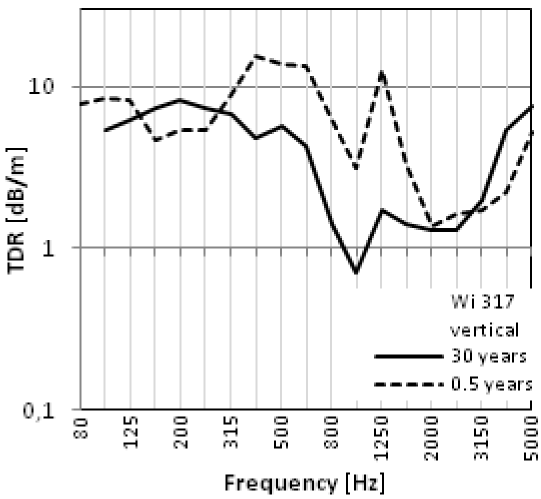


Figure 2 Vertical TDRs of worn and new rail pads

It can be seen that the horizontal decay rates are nearly unchanged whereas the vertical decay rates vary considerably, particularly between around 300 Hz and 2 kHz. The vertical TDRs of the 30 year old are lower than would be expected from a 'stiff' pad.

Interesting results about radiated noise of these two situations of track can be found by using the STARDAMP Tool [2] for noise calculation of the undamped track using the measured decay rates

Table I. Comparison of predicted noise sound power level based on decay rates with old and new pads.

| | 30 years old rail pad | 0.5 years old rail pad |
|---|---|---|
| Freight 80km/h | 102.6 dB(A) | 100.7 dB(A) |
| Regional 120 km/h | 110.3 dB(A) | 107.6 dB(A) |

Comparing the noise radiation of new and old rail pads for freight trains running at 80 km/h the difference is about 1.9 dB(A). For regional passenger trains at 120 km/h the difference increases up to 2.7 dB(A). The decrease of the rail pad stiffness results in a lower coupling of the rail with the sleeper resulting in an increase in the noise level of the track.

## 3. STUVA test rig servo hydraulic engine

The tests at the STUVA laboratories used a nearly rectangular time signal at a frequency of about 2 Hz to load the pads (see Figure 3). This signal was chosen as it was felt to better represent the loading of a train than the conventional sinusoidal signal defined in EN 13146-9 [3]. The frequency approximates to the axle passing frequency of a train travelling at 80 km/h; the loading is representative of axle loads up to 23 t.

The compression of the rail pad was measured using two LVDTs positioned at each end of a section of rail. In Figure 4 the setup of the test rig is shown while Figure 4 shows a time window of the load signal. During the measurement of each rail pad, the maximum load per duty cycle was slowly increased over time from around 0 kN up to 115 kN (Figure 5). These diagrams visualise some features relating to the test rig and also the elastomers. It can be seen that the servo hydraulic engine overshoots the target maximum load particularly at low loads. However, it is not expected that this effect has a large influence on the results. The other feature is that the relaxation behaviour of elastomers leads to the fact that during the release process of the load, the rail pad does not fully recover. This is similar to real track conditions, for the repeated loading/unloading related to the axles passing.

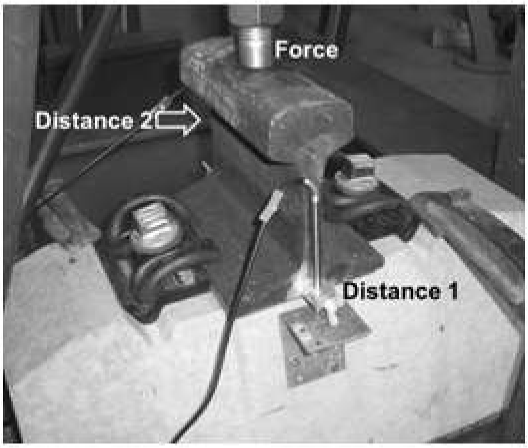


Figure 3 Test rig at STUVA laboratories – sleeper and clamped rail und servo hydraulic engine

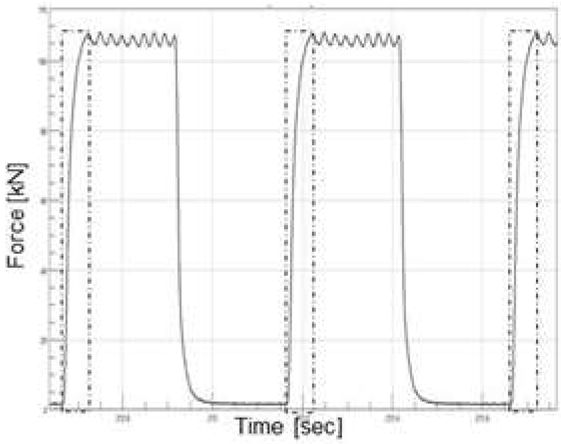


Figure 4 Time window of the load signal of the servo hydraulic engine

The measured data allows the analysis of the rail pad stiffness in two ways. If only the rising edge of the force signal (indicated by dashed lines in Figure 5) and corresponding compression signals are taken for analysis, the stiffness of the rail pad can be calculated by a simple division of actual load by actual compression. This method is compatible with the analysis mentioned in EN 13146-9 for quasi-static measurements. The results are shown in Figure 7.

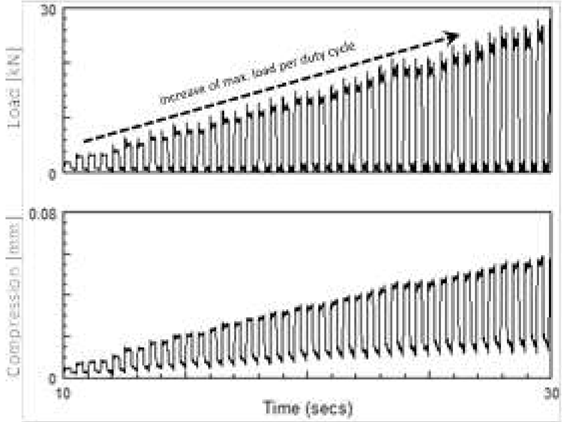


Figure 5 Increase of load per duty cycle and resulting increase of the compression (here average of both sensors)

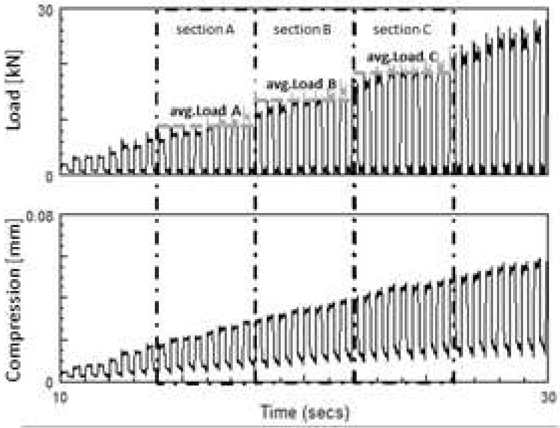


Figure 6 Separation of the full run-up into several time windows (section…) for a frequency analysis of the rail pad stiffness

The method described above will supply stiffness data for every load, but no information about the change of stiffness over frequency. A frequency response function (FRF) calculation can be made to derive this information. The FRFs are calculated over five sections of the full run, each covering several load cycles (e.g. Figure 6). Each analysed section results in a frequency dependent stiffness of the rail pad, but only for discretised loads, calculated as the average load during each time section. The choice of the window length defines the frequency resolution; a window length of 5 seconds was used. Figure 8 compared the frequency dependent stiffness for three different rail pads at an averaged load of about 30 kN. The dynamic stiffness derived using this method is consistently higher than the quasi-static stiffness derived using the method described above (in Figure 7).

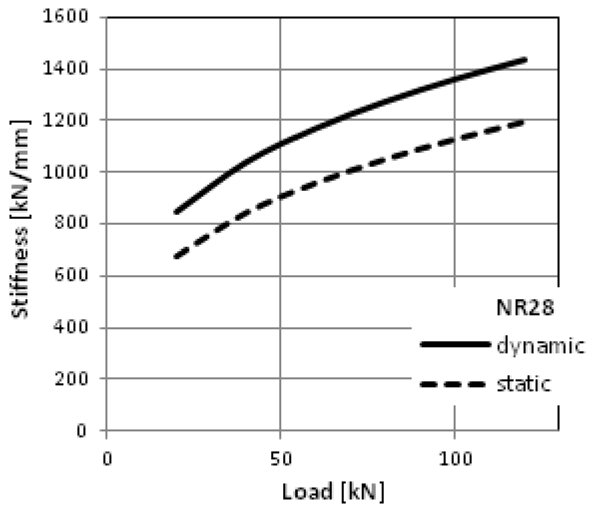


Figure 7 Quasi-static stiffness and dynamic stiffness of an unworn rail pad

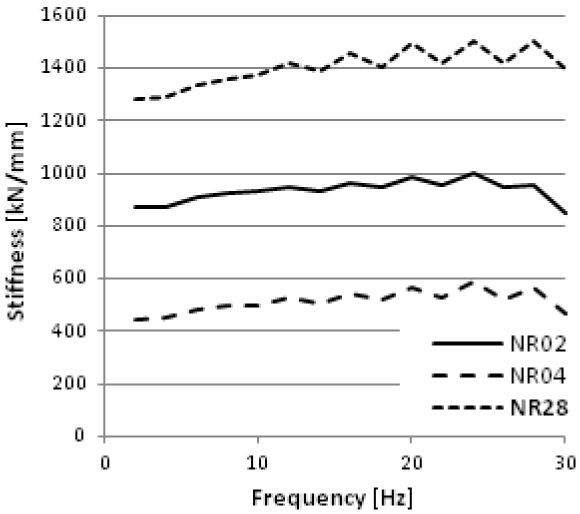


Figure 8 Frequency dependent stiffness of three different rail pads analyzed from servo hydraulic engine

## 4. Re-calculation of pad stiffness via analytical models by the use of TDR data

As an alternative, pad stiffness can also be derived by fitting analytical models to measured data. Here, an analytical model of a track is optimised to give a best fit to the decay rates measured on track.

This analytical model solves the wave propagation problem illustrated in Figure 9. It consists of an infinite Timoshenko beam supported by a two-layer foundation. Sleepers are modelled as flexible bodies as in [1]. For a given force, two different waves are travelling on each side of it, a propagating one, characterised by a wavenumber $k_p$, and a decaying one, with wavenumber $k_e$. Once these wavenumbers are obtained, decay rates can be computed from the imaginary part of the propagating wave as [1]:

$$TDR = -8.6861\, Im(k_p) \qquad (1)$$

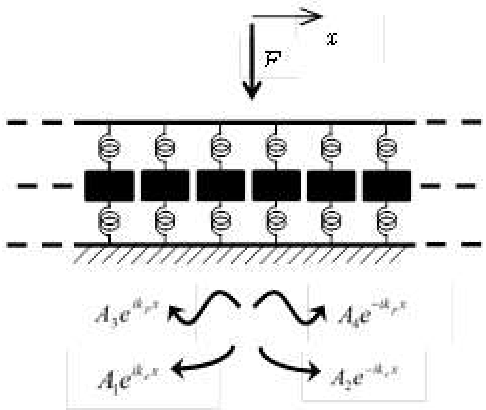


Figure 9 Schematic representation of waves travelling in an infinite beam on a two-layer foundation

Alternatively, a full solution of the forced problem can give the transfer mobilities along the rail and the procedure of standard EN15461 [4] can be applied to obtain the TDR. The two methods give similar results and the first one is adopted for this study. Examples of TDR obtained with this model for different values of pad stiffness are shown in Figure 10. The increase of decay rate with pad stiffness is clearly highlighted in this figure. The fluctuations characterising the results for pad stiffness above 300 MN/m are due to the bending modes of the sleeper; they would be less pronounced in a on-third octave band representation.

Within the curve fitting algorithm the rail pad stiffness ($s_p$) and loss factor ($\eta_p$) are given an initial value of 100 MN/m and 0.2, respectively. A nonlinear least squares curve fitting problem is solved having the form of:

$$\min_{(s_p,\eta_p)} \left\| f(s_p,\eta_p) \right\|_2^2 = \min_{(s_p,\eta_p)} \left( \sum_{i=1}^{n} f_i(s_p,\eta_p)^2 \right) \qquad (2)$$

where the objective function $f$ represents the difference between measured and calculated decay rate in each one-third octave frequency band $i$.

From Figure 10 it is clear that the strong effect of pad stiffness on decay rate is at frequencies below 1-2 kHz. The stiffness also defines the frequency region where a transition occurs between high and low decay rates. This can be at about 200 Hz for soft pads (100 MN/m) and up to 1 kHz for stiff pads (1000 MN/m). At higher frequencies other track properties not included in the model – such as the pinned-pinned resonance, rail damping and higher order waves – determine the main trend of the decay rates. For this reason the curve fitting procedure is performed only between the frequency bands centred at 100 Hz and 1 kHz (or 2 kHz for very stiff pads). An example of a fitted TDR is compared with the corresponding measurement in Figure 11. In this case pad stiffness is estimated at around 200 MN/m.

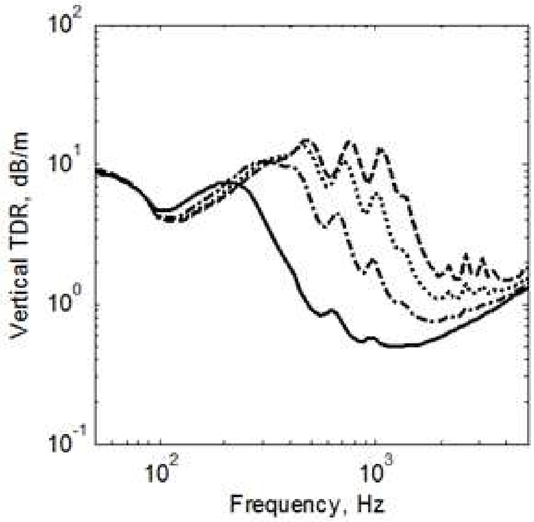


Figure 10 Examples of analytical calculations of TDR. --, sp= 100 MN/m; -.-., sp= 300 MN/m;......, sp= 600 MN/m; -- -- -- sp= 1000 MN/m

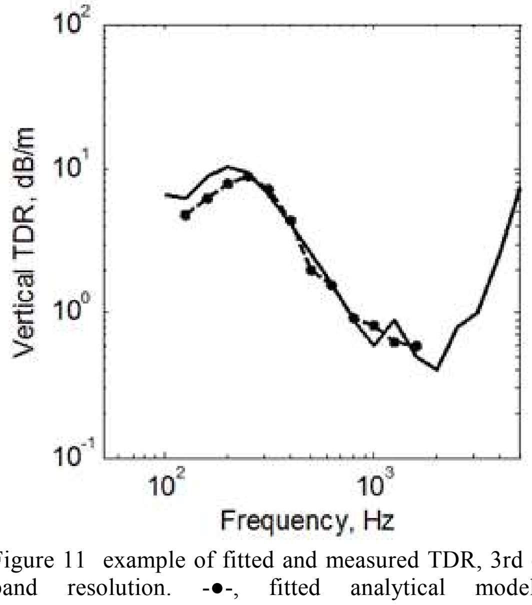


Figure 11 example of fitted and measured TDR, 3rd octave band resolution. -●-, fitted analytical model; --, measurements.

## 5. Pad stiffness versus summed axle load

Some caution should be taken when comparing the results of the two ways of deriving the rail pad stiffness, tests in the laboratory by use of dismounted rail pads and re-calculation from TDR data. The stiffness derived via the analytical model is a best fit to the decay rates over a wide frequency range (100 Hz – 1 KHz) while the stiffness derived from the measurements on the test rig is only valid at frequencies up to 30 Hz. This is due to limits on the rising time of the force at high loads. To bridge this gap, a regression analysis of the FRF-data at 20 kN was carried out to give an indication of the pad stiffness at 800 Hz. Figure 12 shows that the stiffness values derived from both methods are very similar.

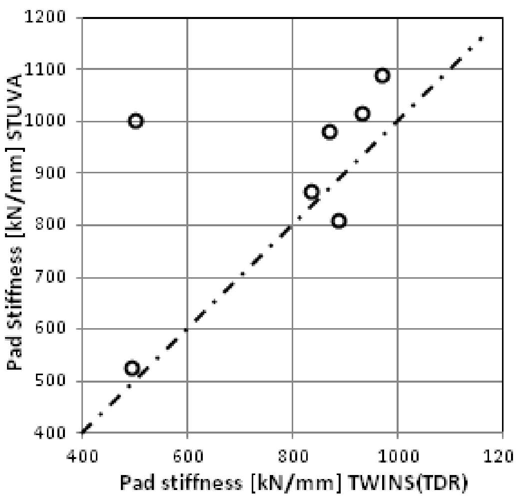


Figure 12 Comparison of pad stiffness developed at servo hydraulic engine and re-calculation from TDR-data

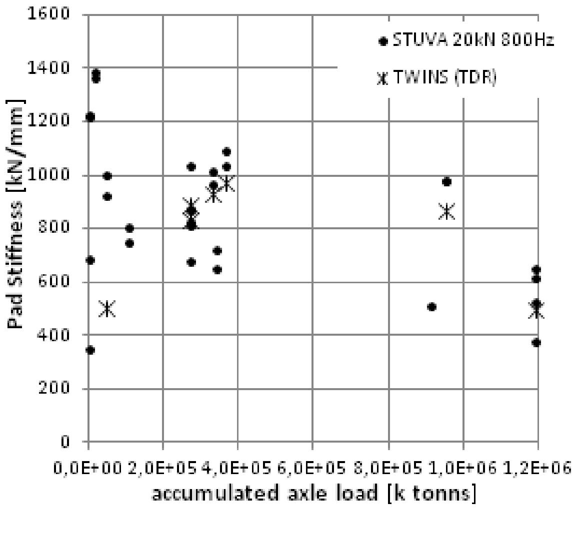


Figure 13 Comparison of pad stiffness vs. accumulated axle load for stiffness' derived in the STUAVA laboratory and from TDRs

SBB provided data about the installation date of the rail pads and an estimate of the accumulated averaged annual axle load across tested tracks. From this additional data it is possible to compare the pad stiffness over the accumulated axle load (figure 13).

Figure 13 suggests that pad stiffness may decrease with accumulated axle load. This effect could account for the differences in TDR between the nominally similar new and old rail pads at the same location. A similar finding was observed by Kaewunruen and Remennikov [5], who suggested a linear deterioration of the stiffness of about 2.18 kN/mm at an accumulated axle load of 1 MGT whereas the results from the work here suggest a deterioration of about 3.06 kN/mm. A linear regression is not suitable for describing the changes over wear. Additional studies are necessary for better understanding.

An alternative explanation for the apparent reduction in pad stiffness over time (or wear) is that the constraint conditions of the pad in the clipping assembly changes over time. For instance the clamping force could reduce due to a reduction in thickness of the pads, or the constraint at the edges of the pads within the assembly reduces. Further investigations are required to explore whether any changes of the pad properties over time are associated with a direct change in the material properties or indirect variations due to changes in the clipping force or constraint conditions.

## 6. Conclusion and outlook

The results suggest that the variation in decay rates of sections of Swiss railway track with nominally similar rail pads fitted may be explained by ageing (or wear) of the rail pads. The results show that pad stiffness tends to decrease with increased accumulated axle load. This decrease of stiffness is predicted to result in an increase in radiated noise. It is not known whether this is due to a change in material properties or a change in the constraint conditions within the rail clip.

Further work is required to substantiate this finding and to improve the understanding of the mechanisms of rail pad ‘ageing’ and their effect on decay rates and noise.

## Acknowledgement

The authors gratefully acknowledge the SBB for commissioning the work. Funding for the project was supplied by the Swiss Federal Office for Transport

## References

[1] D.J.Thompson, Railway Noise and Vibration; Elsevier Oxford 2009

[2] STARDAMP-Tool, calculation software developed during R&D-projekt STARDAMP, 2010-2012 funded by the DEUFRAKO

[3] EN 13146-9 Railway applications - Track - Test methods for fastening systems - Part 9: Determination of stiffness; EN 13146-9:2009+A1:2011

[4] EN 15461 Railway applications — Noise emission — Characterisation of the dynamic properties of track sections for pass by noise measurements

[5] S. Kaewunruen, A.M. Remennikov, RESPONSE AND PREDICTION OF DYNAMIC CHARACTERISTICS OF WORN RAIL PADS UNDER STATIC PRELOADS,14th congress of sound and vibration ICSV14, 9 – 12 July, Cairns Australia